Kidney International, Vol. 61 (2002), pp. 1475–1485

Podocytopenia and disease severity in IgA nephropathy

KEVIN V. LEMLEY, RICHARD A. LAFAYETTE, MASSY SAFAI, GERALDINE DERBY, KRISTINA BLOUCH, ADDY SQUARER, and BRYAN D. MYERS

Division of Pediatric Nephrology, and Division of Nephrology, Stanford University School of Medicine, Stanford, California, USA

Podocytopenia and disease severity in IgA nephropathy.

Background. IgA nephropathy is a common form of progressive glomerular disease, associated with proliferation of mesangial cells and mesangial deposition of IgA. The present study was designed to investigate functional and morphological covariates of disease severity in patients with IgA nephropathy.

Methods. Glomerular hemodynamics, permselectivity and ultrastructure were studied in 17 adult patients with IgA nephropathy using inulin, para-aminohippuric acid (PAH) and ^{3}H-Ficoll clearances and morphometric methods. A mathematical model of macromolecule permeation through a heteroporous membrane was used to characterize glomerular permselectivity. Controls consisted of 14 healthy living kidney donors and 12 healthy volunteers.

Results. The patients were heterogeneous in their disease severity, but as a group had a decreased glomerular filtration rate (GFR) and increased urinary protein excretion compared to controls [63 ± 29 SD vs. 104 ± 23 mL/min/1.73 m^2, $P < 0.001$, and (median) 1.34 vs. 0.11 g/day, $P < 0.0001$, respectively). A multivariate analysis of structural and functional relationships revealed GFR depression to be most strongly correlated with the prevalence of global glomerular sclerosis ($t = -4.073$, $P = 0.002$). Those patients with the most severe glomerular dysfunction had a reduced number of glomerular visceral epithelial cells (podocytes) per glomerulus. The degree of podocytopenia was related to the extent of glomerular sclerosis and of impairment of permselectivity and GFR, with worsening injury below an apparent threshold podocyte number of about 250 cells per glomerulus. There were no corresponding correlations between these indices of injury and the number of mesangial and endothelial cells.

Conclusions. Our findings show that podocyte loss is a concomitant of increasing disease severity in IgA nephropathy. This suggests that podocyte loss may either cause or contribute to the progressive proteinuria, glomerular sclerosis and filtration failure seen in this disorder.

Key words: glomerulus, morphometry, proteinuria, GFR, end-stage renal disease, progressive glomerular disease, filtration failure, podocytes.

Received for publication June 4, 2001
and in revised form October 23, 2001
Accepted for publication November 2, 2001

IgA nephropathy is the most common form of primary glomerular nephritis in children and young adults worldwide. Although variable clinically, the disease is characterized by mesangial deposits of IgA associated with mesangial cell proliferation, hematuria that is often intermittent, and proteinuria that is usually mild. An often insidious progression to end-stage renal failure in 25 to 40% of cases is accompanied by the development of glomerular sclerosis [1]. D'Amico has proposed functional and structural predictors for the development of end-stage renal failure based on his analysis of several studies using Kaplan-Meier survival curve methodology [2]. These predictors include azotemia, heavy proteinuria and hypertension at the time of diagnosis, along with tubulointerstitial damage and glomerular sclerosis on the diagnostic biopsy. Other studies also have shown heavy initial proteinuria, a decreased glomerular filtration rate (GFR) at diagnosis, the presence of crescents, loss of glomeruli and peripheral capillary wall staining with IgA to be predictors of a poor prognosis [1, 3].

The slow rate of progression in most cases of IgA nephropathy has made studies of both prognostic factors and potential therapies difficult. As with other glomerular diseases, the process of progression reflects a complex interplay of both functional and structural components. Loss of glomerular filtration capacity, impaired macromolecule permselectivity, and irreversible structural changes (glomerular sclerosis, interstitial fibrosis) all represent aspects of disease progression. An understanding of the mechanisms involved in these processes may be expected to aid both with the determination of prognosis and in guiding the development of new therapies.

To better understand the pathogenesis of disease progression, we performed an analysis of glomerular function and structure in 17 adult patients with biopsy-proven IgA nephropathy of recent onset. We used a combination of physiologic and morphometric techniques to characterize those changes in the intrinsic properties of the glomerular capillaries that underlie the development of proteinuria and the depression of GFR. Our findings form the basis of this report.

METHODS

Patients

The subjects were 17 adult patients diagnosed by biopsy within the three years preceding their enrollment in this study. The median age was 40 years (range 24 to 64 years) and 10 subjects were male. Other causes of IgA-positive glomerular staining, such as Henoch-Schönlein nephritis and lupus nephritis, were excluded. The majority of patients (15 of 17) were taking antihypertensive medications [in all but one case including an angiotensin-converting enzyme (ACE) inhibitor or angiotensin receptor blocker] and six patients were taking fish oil supplements (4 to 12 g/day) at the time of their physiologic studies.

Control subjects for the morphologic analyses were 14 normal, healthy kidney transplant donors who had intraoperative renal biopsies taken at the time of donation. Controls for the physiologic studies were a separate group of 12 healthy volunteers with no history of renal disease or diabetes. Each was found on examination to be normotensive and to have no proteinuria by dipstick. The median age for the structural control subjects was 42 years (range 23 to 55 years) and for the functional controls was 25 years (range 22 to 40 years). Five of the structural controls and seven of the functional controls were male.

Patients and volunteers were admitted to the General Clinical Research Center at Stanford University Hospital for their clearance studies. The study protocol was approved by the Stanford University Administrative Panel on Human Subjects in Medical Research. Written informed consent was obtained from all participating patients and volunteers.

Glomerular function

Glomerular filtration dynamics were examined during water diuresis by way of timed urinary clearances of inulin and p-aminohippuric acid (PAH). After an intravenous loading dose of inulin (50 mg/kg) and PAH (12 mg/kg), a constant infusion of these markers was administered to maintain constant plasma concentrations. After a 60-minute equilibration period, four timed urine collections were made at 20-minute intervals with plasma samples taken to bracket each urine collection. The average of four urinary inulin clearances was considered to represent the GFR. The renal plasma flow rate was derived by dividing the urinary PAH clearance by an estimated arteriovenous extraction ratio of 0.7 in those patients with a GFR less than 80 mL/min · 1.73 m^2 and by a ratio of 0.8 in those patients with a GFR greater than 80 mL/min · 1.73 m^2 [4]. The renal plasma flow rate in healthy controls was derived using an estimated extraction ratio of 0.9. Urine and plasma PAH and inulin concentrations were determined with an autoanalyzer technique [4]. Plasma oncotic pressure was determined by membrane osmometry [5]. Urine and plasma concentrations of albumin and immunoglobulin G (IgG) were determined by immunochemical techniques [6]. The fractional clearances (θ) of albumin and IgG were determined as the urine-to-plasma concentration ratio of the protein divided by the corresponding concentration ratio of inulin. Urinary protein excretion was determined by routine clinical methods using the pyrogallol red assay.

Glomerular permeability

Because it behaves as a rigid sphere during transglomerular permeation, thereby providing an adequate estimate of the effective glomerular pore sizes presented to circulating globular proteins, we selected Ficoll as a macromolecular probe of the filtration barrier [7]. Ficoll 70, a polymer of sucrose, was provided by Pharmacia LKB Biotechnology (Uppsala, Sweden) and tritiated as described previously [7]. A total of 1.5 mCi of ^{3}H-Ficoll 70 was infused as a bolus at the end of the equilibration period for inulin and PAH. The component molecules of Ficoll 70 span a range of Stokes-Einstein radii from 10 to 100 Å [7]. The sieving coefficients of Ficoll molecules of graded size were determined after separation of urine and serum into narrow fractions by size-exclusion chromatography as previously described [7]. Briefly, the ^{3}H-labeled Ficoll 70 was separated by high-pressure liquid chromatography (HPLC) using Ultrahydrogel 500 and 250 columns in series (Waters, Milford, MA, USA). The mobile phase was 0.1 mol/L potassium phosphate, pH 6.5, with a flow rate of 0.5 mL/min. The system was calibrated with five narrowly dispersed Ficoll fractions of known molecular weight (Pharmacia LKB Biotechnology). Serum samples were first diluted 1:1 with distilled water; urine samples were concentrated threefold using a centrifugal concentrator (Speed Vac, Savant Instruments, Farmingdale, NY, USA). Samples were subsequently centrifuged through 0.2 μm cellulose acetate filters (Rainin Instruments, Woburn, MA, USA) and a 200 μL aliquot injected onto the columns. During the interval corresponding to retention times of 26.5 to 38 minutes, 185 μL fractions of the eluent were collected, combined with 3 mL of Cytoscint-ES scintillation fluid (ICN Biomedicals, Irvine, CA, USA) and counted for 10 minutes on a scintillation counter (Tri-Carb 4530; Packard Instruments, Downers Grove, IL, USA). Ficoll molecules in these eluted fractions spanned a molecular radius range of 12 to 92 Å. Fractions collected from 14 to 15.2 minutes did not contain Ficoll and were used to estimate background; their average counts were subtracted from the subsequent fractions. The fractional clearance for each fraction was determined by dividing the urine-to-serum concentration ratios (measured as cpm ratios) for that fraction by the corresponding concentration ratio of inulin. Since neither Ficoll nor inulin

are reabsorbed or secreted by the tubule [8], the fractional clearance for a given size of Ficoll is the same as the glomerular sieving coefficient (Bowman's space/plasma concentration ratio).

Computations based on pore theory

Glomerular permeability to neutral macromolecules was analyzed using a hydrodynamic model of hindered solute transport through a heteroporous membrane [9]. In this model, the major portion of the capillary wall is considered to be perforated by cylindrical, restrictive pores with a lognormal distribution of pore radii. The distribution is characterized by the mean pore radius (u) and a parameter (s) representing the breadth of the pore distribution, where ln(s) is the standard deviation of the distribution of ln(r), with r the pore radius. A second population of large, nonrestrictive pores serves as a parallel "shunt" pathway. The quantitative representation of the latter is by the shunt parameter (ω_0), which specifies the fraction of the total glomerular filtrate passing through the nonrestrictive portion of the membrane. The heteroporous (lognormal + shunt) model was fitted to the ^{3}H-Ficoll sieving data (from 14 Å radius to the largest radius measurable) of the individual patients using the nonlinear least squares method. The model also requires information on the filtration dynamics of the glomerulus, including the GFR, renal plasma flow, plasma oncotic pressure and the glomerular transcapillary hydraulic pressure difference. Since the latter cannot be directly determined in humans, a value of 46 mm Hg was assumed [7, 9, 10].

Morphometry

The renal biopsy was performed within a median time interval of 15 months (range 2 to 54 months) from the clearance study. Biopsy was performed using a 18 G biopsy needle (Monopty, Bard, Covington, GA, USA). Core fragments were fixed in Zenker's solution or 2% paraformaldehyde/2.5% glutaraldehyde in 0.1 mol/L cacodylate buffer. The former were then embedded in paraffin, cut and stained for light microscopy, and the latter were embedded in LX112 resin (Ladd Research Industries Inc., Williston, VT, USA), cut and stained for electron microscopy.

The volume of patent and segmentally sclerotic glomeruli was estimated from the planar area of the glomerular profiles in single sections of paraffin-embedded tissue using the method of Weibel [11]. The average number of profiles examined per individual was 9.5 (range 3 to 23). Final volume was corrected for the effects of paraffin embedding [12]. The fraction of globally sclerotic glomeruli was estimated from review of the single sections. A glomerulus was considered globally sclerotic if no patent capillary lumina were noted in the profile. The estimated frequency of global sclerosis was adjusted to compensate for the decreased probability of sampling these glomeruli, which are smaller than patent glomeruli, using the following formula:

$$\%GS = \frac{N_s}{N_s + N_p \cdot (D_s/D_p)} \times 100 \qquad \text{(Eq. 1)}$$

where %GS is the fraction of glomeruli manifesting global glomerular sclerosis, N_s is the number of globally sclerotic glomerular profiles in the biopsy sections, N_p is the number of patent glomerular profiles in the sections, D_s is the mean diameter of the sclerotic glomeruli and D_p is the mean diameter of the patent glomeruli. Fractional interstitial area (FIA) was estimated by point counting through the microscope ocular on paraffin-embedded material. To avoid bias, "forbidden" edges of the ocular grid were excluded from the counting frame [13]. Adequate material was available for calculation of the percentage of glomeruli with global sclerosis and the fractional interstitial area in seven control subjects.

Photomontages of one to two complete glomerular profiles (magnification ×2880) chosen at random were used to determine the filtration surface area density, mesangial volume density, and podocyte and endocapillary cell densities using standard methods [11]. The number density of glomerular cells was estimated using the formula [11]:

$$N_v = \frac{1}{\beta} \cdot \sqrt{\frac{N_A^3}{A_A}} \qquad \text{(Eq. 2)}$$

where N_V is the number density of cells per μm^3 of tuft volume; N_A is the number of intersections of cell nuclei per μm^2 of tuft area; A_A is fractional areal density of the nuclei; β is the shape factor for prolate ellipsoids, which has the value of 1.65 for podocytes and 1.56 for endocapillary cells (that is, endothelial plus mesangial cells) [14]. The density of endocapillary cells was estimated rather than that of mesangial and endothelial cells separately, since a clear distinction between these two cell types is not always possible even at high magnification. The total number of podocytes and endocapillary cells per glomerulus was obtained by multiplying the number density for each cell type by the mean glomerular tuft volume. Higher-power prints (×11,280) from these glomeruli were used for the determination of the thickness of the glomerular basement membrane (GBM) by the orthogonal intercept method of Jensen, Gundersen and Østerby [15] as well as the harmonic mean foot process width after correction for the effects of sectioning angle [16]. The same high-power micrographs were used to estimate the frequency of epithelial cell filtration slits, defined as the number of slits per millimeter of GBM length. Suitable material for electron microscopy was not available for three patients, limiting the ultrastructural portion of the morphometric analysis to 14 patients with IgA nephropathy.

Table 1. Glomerular function

Group	IgA nephropathy	Control	*P*
GFR *mL/min/1.73 m²*	63 ± 29	104 ± 23	<0.001[a]
Renal plasma flow *mL/min/1.73 m²*	402 ± 149	623 ± 193	0.002[a]
Filtration fraction *%*	15 ± 4	17 ± 3	NS
Plasma oncotic pressure *mm Hg*	23 ± 3	26 ± 2	<0.001[a]
Mean arterial pressure *mm Hg*	95 ± 11	85 ± 10	0.022[a]
Proteinuria[b] *g/24 h*	1.34 (0.15–4.69)	0.11 (0.06–0.26)	<0.001[c]
θ-albumin[b] *×10⁻⁵*	37.9 (0.4–422)	0.2 (0.1–1.3)	<0.001[c]
θ-IgG[b] *×10⁻⁵*	6.2 (0.4–125)	0.2 (0.1–0.7)	<0.001[c]

Abbreviations are: GFR, glomerular filtration rate; θ-albumin, fractional clearance of albumin; θ-IgG, fractional clearance of IgG.
[a] *t* test
[b] Median (range)
[c] Mann-Whitney test

Calculation of single-nephron ultrafiltration coefficient

The single-nephron ultrafiltration coefficient (SNK_f) was calculated as the product of the total anatomic surface area available for filtration and the intrinsic hydraulic permeability of the glomerular capillary wall. The filtration surface area was calculated as the product of the surface area density determined from the electron micrographs and the mean glomerular tuft volume. In this calculation, we corrected both for the effects of paraffin embedding and for the decreased glomerular dimensions resulting from immersion fixation compared to fixation in situ [12].

The hydraulic permeability (k) was estimated using the hydrodynamic model of Drumond and Deen [17]. Briefly, the hydraulic permeability of the glomerular capillary wall is the inverse of the hydraulic resistance of that structure. This resistance may be calculated as the sum of the series resistances of the three components of the glomerular capillary wall, viz. the endothelial layer, the GBM and the epithelial layer. Thus,

$$k = \left(\frac{1}{k_{endo}} + \frac{1}{k_{GBM}} + \frac{1}{k_{cpi}}\right)^{-1} \qquad \text{(Eq. 3)}$$

where k_{endo}, k_{GBM} and k_{epi} are the hydraulic permeabilities of the endothelial layer, the GBM and the epithelial layer, respectively. As described elsewhere [10, 16], the component resistances are derived in part from structural measurements made in the rat and in part from measurements made in the IgA nephropathy patients and normal control subjects of the present study. In particular, the values for the endothelial layer permeability k_{endo} (2.0×10^{-7} m/s/Pascal), the filtration slit diaphragm permeability k_s (7.9×10^{-8} m/s/Pascal), the filtration slit diaphragm width (W_s; 41 nm) and the Darcy permeability of the glomerular basement membrane material K_D (2.7 nm²) were derived from studies in the rat [17]. The value for k_{GBM} was calculated from K_D and from the basement membrane thickness and the filtration slit frequency measured in the human subjects using the same model. The permeability of the epithelial layer k_{epi} was calculated from k_s, the slit diaphragm width W_s and from the filtration slit frequency measured in the human subjects.

Statistics

Results are reported as mean ± standard deviation or median (range). Differences between groups were evaluated by *t* test or Mann-Whitney test. Correlation between variables was by least-squares linear regression. Multivariate regression of the three cardinal markers of disease severity (GFR, ω_0, and the percentage of glomeruli manifesting global sclerosis) on potential explanatory variables was based on the stepwise procedure. Statistical analysis was performed using SPSS Base 8.0 for Windows (SPSS, Inc., Chicago, IL, USA).

RESULTS

Glomerular function

Results of glomerular function assessments of patients and controls are shown in Table 1. The IgA nephropathy patients had on average a lower GFR (63 ± 29 vs. 104 ± 23 mL/min/1.73 m², $P < 0.001$) and renal plasma flow (402 ± 149 vs 623 ± 193 mL/min/1.73 m², $P = 0.002$) than the control subjects, although three of the 17 patients had a GFR of ≥ 90 mL/min/1.73 m² (Fig. 1). Filtration fraction was numerically less in the patients (15 ± 4 vs. 17 ± 3%, P = NS). The patients also had lower plasma oncotic pressures (23 ± 3 vs. 26 ± 2 mm Hg, $P < 0.001$), greater amounts of proteinuria [1.34 (range 0.15–4.69) g/24 h vs. 0.11 (0.06–0.26) g/24 h, $P < 0.0001$] and higher mean arterial pressures (95 ± 11 vs. 85 ± 10 mm Hg, $P = 0.02$).

In accord with the increased urinary protein excretion among the IgA nephropathy patients, their fractional clearances of albumin and IgG exceeded control values by one to two orders of magnitude ($P < 0.001$, Table 1). As with urinary protein excretion, the range of values in the IgA nephropathy group was quite broad, with individual fractional clearances varying over more than

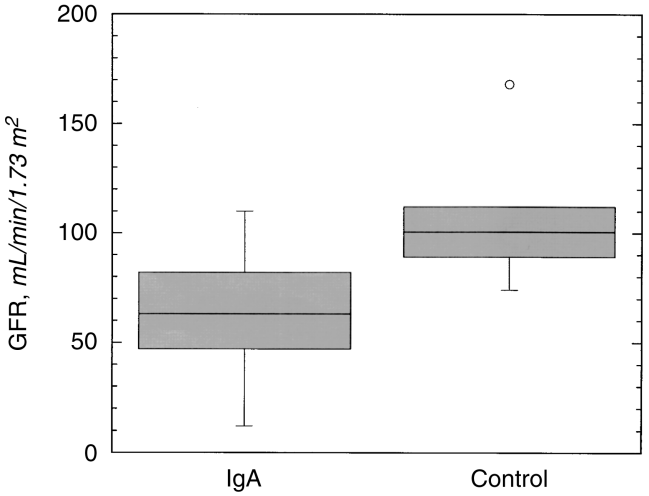

Fig. 1. Glomerular filtration rate (GFR) in the IgA nephropathy (IgA) and control groups.

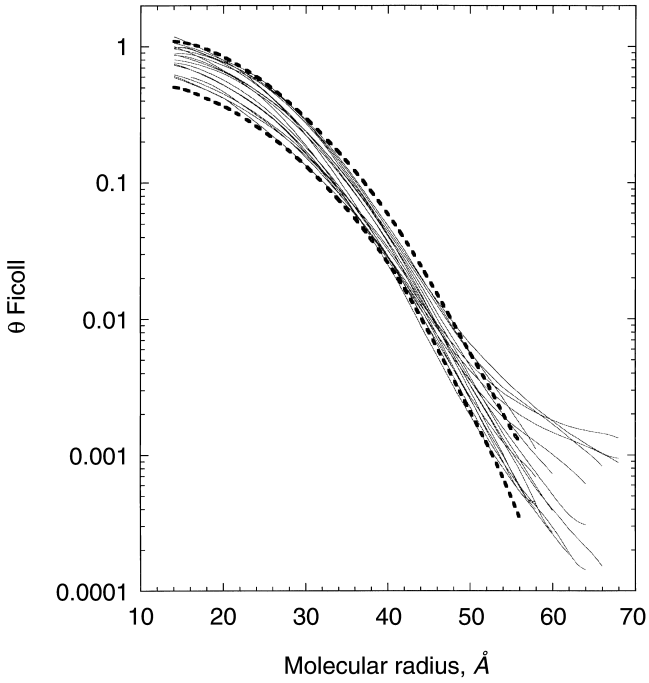

Fig. 2. Ficoll sieving curves in individual patients with IgA nephropathy (thin lines), representing the relationship between the fractional clearance of a given Ficoll and its molecular radius. The normal range for Ficoll sieving curves in our laboratory (2 SD above and below the mean value) is indicated by the two heavy dashed lines. The normal range is limited because urinary Ficoll is usually not detected for molecular radii >56 Å.

two orders of magnitude. Ficoll sieving coefficients in both subjects with IgA nephropathy and controls declined monotonically with increasing molecular radius (Fig. 2). Ficoll sieving curves for the IgA nephropathy patients fell within the normal range for molecular radii up to about 48 Å. In a subset of the patients the sieving curves began to exceed the normal range at molecular radii above this value. Whereas Ficoll fractions of 56 Å were only rarely detectable in the urine of control subjects, fractions of 60 to 70 Å could be detected in the urine of most patients with IgA nephropathy. These abnormalities indicate impairment of the size-selectivity of the glomerular barrier.

Glomerular structure

The percentage of glomeruli exhibiting global glomerular sclerosis was 28 ± 23% in the IgA nephropathy patients and 0% in the control subjects ($P = 0.002$; Table 2). The remaining patent glomeruli in the patients were enlarged as indicated by a mean glomerular tuft volume that exceeded the control value by 40% ($P < 0.05$). The higher frequency of global glomerular sclerosis in the patients was associated with an almost twofold increase in the fractional interstitial area ($P < 0.01$). Matrix accumulation also occurred within the patent glomeruli, leading to a greater basement membrane thickness (457 ± 61 vs. 385 ± 55 nm, $P < 0.005$) and fractional mesangial volume (27 ± 6% vs. 18 ± 4%, $P < 0.001$) than in controls. This expansion of glomerular matrix components was associated with a modest reduction in filtration surface area density in the IgA nephropathy patients, 0.087 ± 0.024 vs 0.105 ± 0.019 $\mu m^2/\mu m^3$ ($P < 0.05$).

Foot process width was similar in the patients with IgA nephropathy and controls, 425 ± 76 vs. 438 ± 36 nm, respectively (P = NS). The number of visceral epithelial cells (podocytes) also did not differ significantly between the groups, although it tended to be lower in the patients than in controls (238 ± 147 vs. 300 ± 107 cells/glomerulus, $P = 0.10$). In contrast, the average number of endocapillary (mesangial plus endothelial) cells per glomerulus was significantly greater in the IgA nephropathy patients than in controls (1268 ± 595 vs. 852 ± 350 cells/glomerulus, $P < 0.04$).

Membrane properties

Intrinsic membrane properties of the glomerular capillary wall are summarized in Table 3. On the basis of the log normal + shunt model, patients with IgA nephropathy showed no differences from controls in the mean pore radius (u) or the breadth (s) of the radius distribution of the restrictive pores. By contrast, they did have a much larger fraction (ω_0) of their filtrate permeating the large and nonselective, shunt-like pores (3.57 ± 3.17 vs. 0.36 ± 0.51×10^{-4}, $P = 0.001$). There was a significant log linear relationship between the magnitude of the macromolecular shunt parameter ω_0 and the fractional clearances of both albumin ($r = 0.72$, $P = 0.001$) and IgG ($r = 0.79$, $P < 0.001$) in the IgA nephropathy patients, suggesting that impairment of barrier size-selectivity might contribute to the proteinuria found in these patients (Fig. 3).

Table 2. Glomerular structure

Group	IgA nephropathy	Control	*P*
Global sclerosis *%*	28 ± 23	0	0.002[a]
Glomerular volume $\times 10^6\ \mu m^3$	2.77 ± 1.11	1.97 ± 0.91	<0.05[b]
Basement membrane thickness *nm*	457 ± 61	385 ± 55	<0.005[b]
Fractional interstital area *%*	27 ± 10	16 ± 4	<0.01[b]
Fractional mesangial volume *%*	27 ± 6	18 ± 4	<0.001[b]
Filtration surface density $\mu m^2/\mu m^3$	0.087 ± 0.024	0.105 ± 0.019	<0.05[b]
Foot process width *nm*	425 ± 76	438 ± 36	NS
Number of podocytes per glomerulus	238 ± 147	300 ± 107	0.10[a]
Number of endocapillary cells per glomerulus	1268 ± 595	852 ± 350	<0.04[b]

[a] Mann-Whitney test; [b] *t* test

Table 3. Membrane parameters

Group	IgA nephropathy	Control	*P*
Mean radius of restrictive pores [*u* (Å)]	39.1 ± 4.4	39.0 ± 3.6	NS
Radius distribution parameter (*s*)	1.18 ± 0.05	1.18 ± 0.03	NS
Fraction of filtrate via shunt (ω_0) $\times 10^{-4}$	3.57 ± 3.17	0.36 ± 0.51	0.001[a]
Filtration surface area (S) $\times 10^5\ \mu m^2$	2.27 ± 0.78	2.01 ± 0.84	NS
Hydraulic permeability (*k*) *m/s/Pa*, $\times 10^{-9}$	2.53 ± 0.50	2.51 ± 0.30	NS
Single nephron ultrafiltration coefficient (SNK_f) *nL/(min · mm Hg)*	6.45 ± 3.05	5.62 ± 2.42	NS

[a] Mann-Whitney test

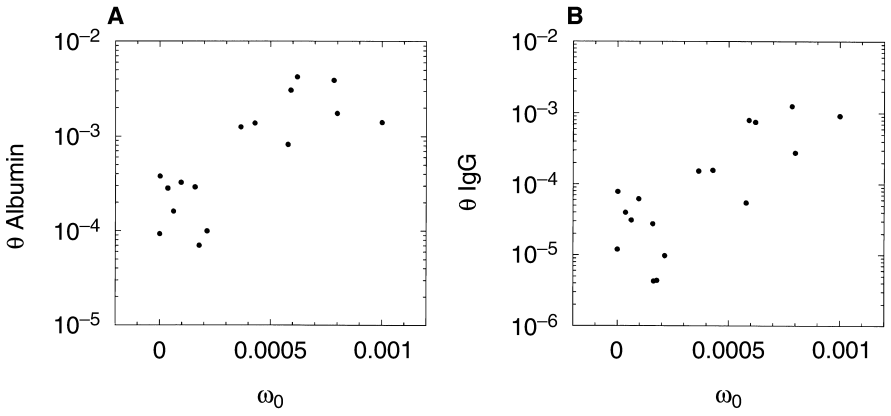

Fig. 3. Relationship between the fractional clearance of albumin (left) and IgG (right) and the fraction of filtrate passing through nonselective shunts (ω_0) in the subjects with IgA nephropathy.

The magnitude of total proteinuria also correlated significantly with ω_0 ($P = 0.016$).

Despite the observed GFR depression, the computed determinants of glomerular ultrafiltration capacity in individual patent glomeruli did not differ between patients with IgA nephropathy and controls. Reflecting an offsetting effect of the larger tuft volumes of the IgA nephropathy patients on their smaller filtration surface area density, the mean glomerular filtration surface area was quite similar in the two groups (2.27 ± 0.78 vs. 2.01 ± 0.84 × 10^5 μm^2; Table 3). The computed hydraulic permeability of the glomerular capillary wall in each group also was not different (2.53 ± 0.50 vs. 2.51 ± 0.30 × 10^{-9} m/s/Pascal), with the result that the calculated single-nephron ultrafiltration coefficient (SNK_f) for the patients was similar to that for controls, 6.45 ± 3.05 vs. 5.62 ± 2.42 nL/(min · mm Hg) (P = NS, Table 3).

Structural-functional relationships

The absence of depression of the ultrafiltration coefficients of the patent glomeruli in IgA nephropathy raised the possibility that obliteration of glomeruli via global sclerosis could represent the major mechanism by which the surface area available for glomerular ultrafiltration, and thus the intrinsic ultrafiltration capacity of the kidney, is reduced in this disorder. That this is likely the case is suggested by a strong inverse relationship between GFR and the percent of globally sclerotic glomeruli ($r = -0.83$, $P < 0.001$; Fig. 4). The only other structural factors that correlated with GFR were the fractional

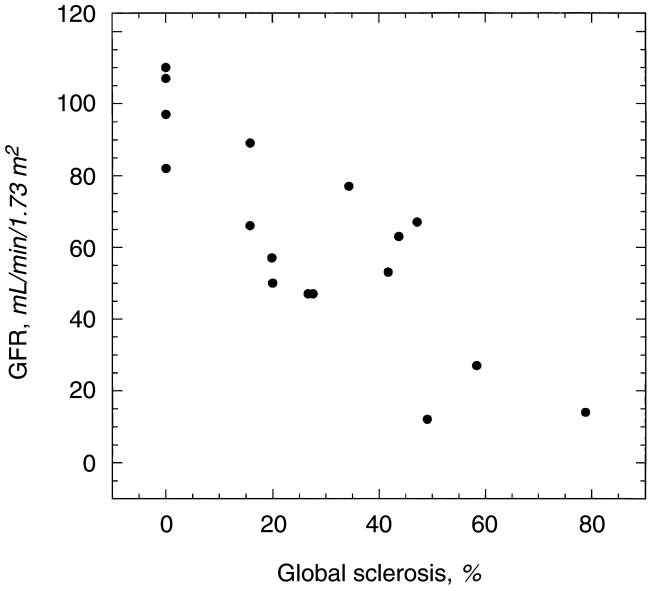

Fig. 4. GFR in the patients with IgA nephropathy plotted against the percent of glomeruli manifesting global sclerosis ($r = -0.83$, $P < 0.001$).

interstitial area ($r = -0.78$, $P = 0.001$) and the number of podocytes per glomerulus ($r = 0.73$, $P = 0.003$). The fractional interstitial area also correlated strongly with the fraction of globally sclerotic glomeruli ($r = 0.80$). We suspect that collagenization and expansion of the interstitium occurs as a result of, and represents a surrogate marker for, glomerular obliteration in this disorder.

Using linear multivariate regression, we analyzed the relationship between GFR and various structural factors (the fraction of glomeruli with global sclerosis, fractional mesangial volume, fractional interstitial area, SNK_f and the numbers of podocytes and endocapillary cells per glomerulus) as well as traditional physiologic determinants of GFR (renal plasma flow, plasma oncotic pressure, and mean arterial pressure). The strongest predictor in the multivariate analysis was the fraction of glomeruli with global sclerosis ($t = -4.073$, $P = 0.002$) followed by the rate of renal plasma flow ($t = 3.137$, $P = 0.009$) and the number of podocytes per glomerulus ($t = 1.990$, $P = 0.075$). In this cross-sectional analysis, GFR was not a function of SNK_f. Despite the significant univariate relationship found between GFR and the fractional interstitial area, the latter did not contribute to the multivariate regression ($t = 0.822$, $P = 0.43$), suggesting that it is indeed a surrogate for the fraction of globally sclerotic glomeruli.

We also investigated the relationships between the above-mentioned structural and physiologic parameters and glomerular permselective function as represented in the magnitude of the nonselective shunt, ω_0. The number of podocytes ($t = -5.843$, $P < 0.001$), plasma oncotic pressure ($t = -6.688$, $P < 0.001$), the fractional interstitial area ($t = 2.813$, $P = 0.02$), and the mesangial volume fraction ($t = -2.578$, $P = 0.03$) showed significant multilinear correlations with the magnitude of the nonselective shunt. Interestingly, there was no apparent relationship between ω_0 and foot process width ($t = 0.644$, $P = 0.538$). The relationship with the plasma oncotic pressure likely represents the development of hypoproteinemia as a result of renal protein losses.

Finally, the relationships of various structural factors (fractional interstitial area, volume of patent glomeruli, percentage of glomeruli with segmental sclerosis, basement membrane thickness, foot process width, the fractional mesangial volume and the numbers of podocytes and endocapillary cells per glomerulus) were examined with the percentage of glomeruli manifesting global glomerular sclerosis. Of these factors, only the fractional interstitial area made a significant contribution to the multivariate regression ($t = 4.554$, $P = 0.001$), although podocyte number was of borderline significance ($t = -2.101$, $P = 0.060$).

Relationship of disease severity with podocyte number within the IgA group

As stated above, significant or nearly significant relationships were found between the number of podocytes and three distinct markers of glomerular injury in the IgA nephropathy group: depressed GFR, the shunt magnitude ω_0, and the frequency of global glomerular sclerosis. Therefore, the nature of these relationships was reanalyzed, as well as those between the endocapillary cell number and these same three markers. Despite a wide range of endocapillary cell numbers per glomerulus in the IgA nephropathy patients, there was no apparent univariate relationship between the number of endocapillary cells and any of the individual markers of disease severity (Fig. 5). In stark contrast, a strong nonlinear relationship emerged between the number of podocytes per glomerulus and each of these markers (Fig. 6). In each case, the marker showed nearly normal values for patients with a podocyte number greater than about 200–250, but then became progressively more deranged as the number of podocytes per glomerulus declined below this apparent threshold value.

DISCUSSION

IgA nephropathy is the most common cause of glomerular nephritis in young adults throughout the world. Although it is often associated with a mild glomerular injury, it can progress to end-stage renal failure in a substantial minority of cases [1, 2]. Reflecting the wide variability of the natural history of this disease, we found the GFR in the subjects of the present study to range from 10 to 110 mL/min/1.73 m^2 (Fig. 1). In an effort to elucidate the mechanism of GFR depression in this

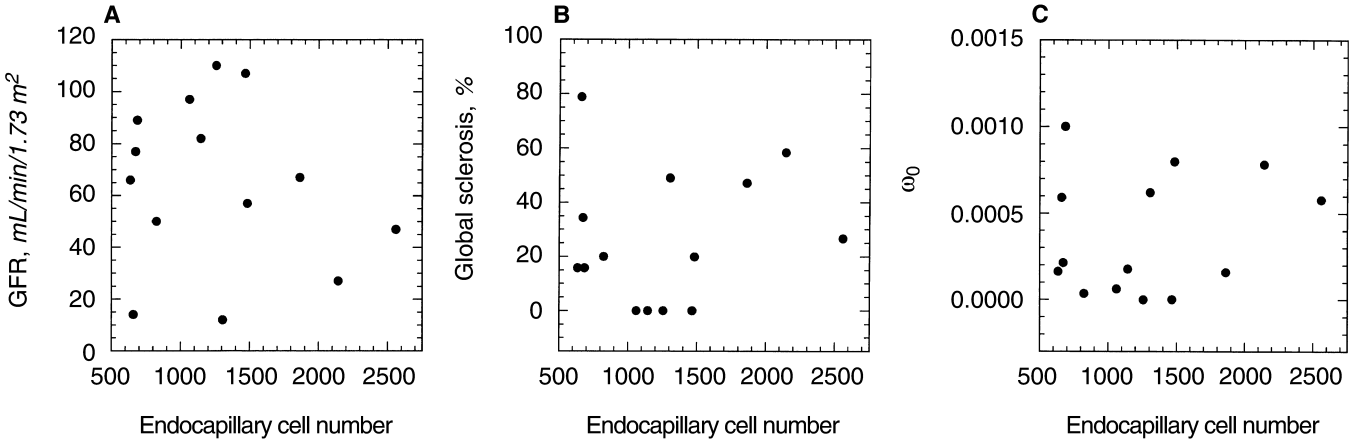

Fig. 5. Relationship of GFR (*A*), percentage of global sclerosis (*B*) and shunt magnitude, ω_0 (*C*) to the number of endocapillary cells per glomerulus in patients with IgA nephropathy.

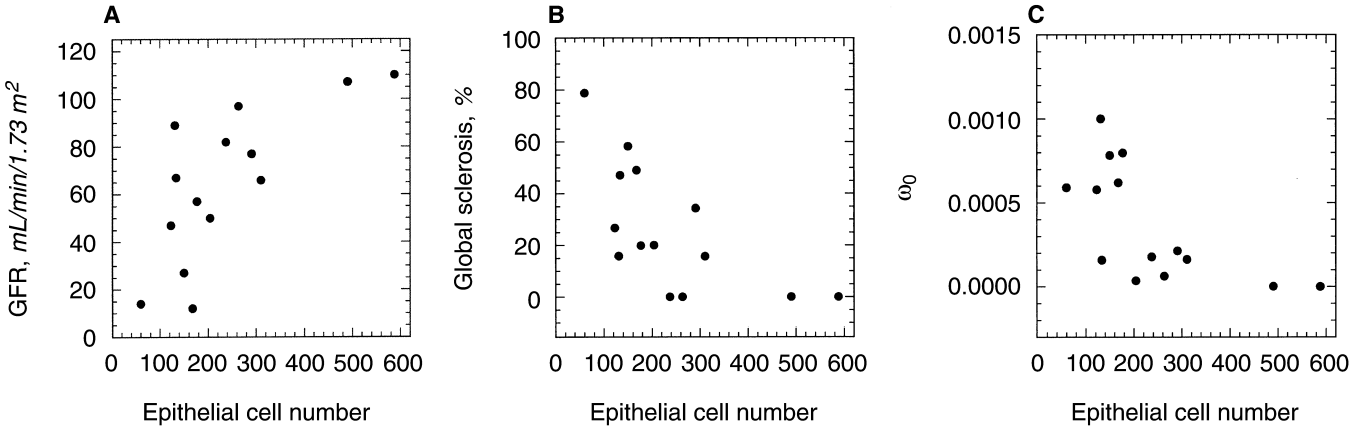

Fig. 6. Relationship of GFR (*A*), percentage of global sclerosis (*B*) and shunt magnitude, ω_0 (*C*) to the number of podocytes per glomerulus in patients with IgA nephropathy.

disorder, we undertook an extensive evaluation of the functional and structural characteristics of the underlying glomerular injury.

The glomerular filtration rate is the product of the net pressure for ultrafiltration across the walls of the glomerular capillaries and the intrinsic ultrafiltration capacity of the aggregate of all of the glomerular capillary tufts in the two kidneys [18]. By linear multivariate analysis, two principal factors that correlated significantly with GFR in the IgA nephropathy patients were identified: the percentage of glomeruli manifesting global sclerosis and the rate of renal plasma flow. The former factor affects the ultrafiltration capacity of the kidneys by decreasing the number of patent, perfused capillary tufts across which filtration can take place, in essence reducing the effective total surface area available for filtration. Although the remnant patent glomeruli underwent compensatory hypertrophy in our patients, there was no significant increase in the filtration surface area per glomerulus, due to a decrease in the filtration surface area density, which may have declined as a result of mesangial expansion. IgA nephropathy was associated with only a small degree of widening of the glomerular basement membrane (457 ± 61 vs. 385 ± 55 nm in controls; Table 2). Similarly, the mean foot process width did not differ from control values. As a result, the hydraulic permeability of the glomerular capillary wall, computed from these quantities using the hydrodynamic model of Drumond and Deen [17], was essentially the same in patients and controls (Table 3). It follows that the single nephron ultrafiltration coefficient (SNK_f) of the patent glomeruli—the product of the filtration surface area and the local hydraulic permeability—was within the normal range in the IgA nephropathy patients and therefore did not contribute to the hypofiltration observed. By exclusion, global sclerosis must be the major, if not the sole, structural determinant of GFR depression in IgA nephropathy.

At first glance, the identification of renal plasma flow as a significant correlate of GFR in the IgA nephropathy patients implies a hemodynamic basis for part of their GFR depression. However, the mechanism by which decreased plasma flow lowers GFR is by elevating the axial concentration profile of the plasma proteins as the blood flows through the glomerular capillaries [19]. Because the oncotic pressure developed by plasma proteins is the force opposing ultrafiltration in the glomerular capillaries, the resulting fall in net ultrafiltration pressure (hydrostatic pressure minus oncotic pressure) with elevation in the plasma protein concentration lowers the GFR. This does not appear to be the case in our IgA nephropathy group, however. On average, the oncotic pressure of plasma entering the afferent end of the glomerular capillary network was 23 mm Hg. From the observed filtration fraction, it was calculated that the mean oncotic pressure of plasma leaving the efferent end of this network was 27 mm Hg. Both values are substantially lower than the corresponding values for the control group (26 and 32 mm Hg, respectively), which should enhance, rather than depress, the net ultrafiltration pressures in IgA nephropathy. We submit that, as in the case of GFR, it is the reduction in the size of the cortical microvascular bed, attendant to the development of glomerular sclerosis and secondary interstitial fibrosis, which accounts for the observed reduction in renal plasma flow. Consistent with this possibility is the similarity of the degree of reduction in renal plasma flow and in the number of patent glomeruli (~30%).

In addition to the depression of GFR, we sought to elucidate mechanisms accounting for abnormal proteinuria and the development of global glomerular sclerosis in IgA nephropathy. The amount of proteinuria was modest, perhaps owing to the use of ACE inhibitors in the majority of patients. In particular, since a very strong association of the fractional clearances of albumin and IgG was found with the magnitude of the nonselective shunt ω_0 (Fig. 3), linear multivariate regressions of ω_0 and the frequency of global sclerosis were performed on putative explanatory structural and functional variables, as the analyses done with GFR.

The analysis of the structural and functional factors correlating with the shunt magnitude ω_0 showed highly significant contributions from the number of podocytes and somewhat weaker contributions from the mesangial volume fraction and the fractional interstitial area. A strong relationship with plasma oncotic pressure likely reflects the influence of urinary protein losses (also significantly associated with the shunt magnitude) on plasma protein concentration. In the case of global glomerular sclerosis, the fractional interstitial area was the only variable with a significant contribution in the multivariate analysis, although the podocyte number made a contribution of borderline statistical significance ($P = 0.06$). In this regard it is interesting that the number of podocytes also had an influence on GFR that was of borderline statistical significance in the multilinear regression ($P = 0.075$). The podocyte number was in fact the only other factor even to come near to achieving statistical significance in the multivariate regression analyses of either GFR or the frequency of global sclerosis. Since the relationship between both GFR and the rate of global sclerosis with podocyte number appears to be nonlinear (Fig. 6 A, B), it is likely that the strength of the multivariate association of podocyte number with these variables is in fact underestimated by using a multilinear regression approach.

The mesangium has usually been regarded as the main target of the immune injury associated with IgA nephropathy. It is in the mesangium that deposits of immunoglobulins and complement accumulate. In the present study, there was an increase in the endocapillary cellularity of the glomerulus, presumably reflecting principally an increase in the number of mesangial cells. There was also an increase in the mesangial volume fraction in IgA nephropathy patients, likely due both to an accumulation of mesangial matrix and to proliferation of mesangial cells. Neither endocapillary cell number nor the mesangial volume fraction, however, correlated with GFR or with the development of glomerular sclerosis. The mesangial volume fraction, but not the number of endocapillary cells, showed a significant correlation with the magnitude of ω_0. In sharp contrast, the number of podocytes per glomerulus was shown by either univariate or multivariate analyses to correlate with all three cardinal markers of disease severity.

When we analyzed the association of podocyte number with the aforementioned three markers of disease severity, a similar relationship was found in each case. Values for the individual marker were close to the normal range for patients with a podocyte number greater than about 200 to 250 cells/glomerulus. As the podocyte number fell below this value, however, the severity of glomerular injury seemed to become progressively worse, so that the overall relationship showed a "threshold" effect (Fig. 6). The significance of the apparent threshold for an effect of the number of podocytes on disease severity is as yet unclear, but it may represent the minimum number of podocytes necessary to maintain the structural stability and functional integrity of the glomerular tuft [20, 21]. Such a relationship could, of course, simply represent a nonspecific correlation among various factors, all of which reflect the severity of glomerular injury. Under this interpretation, loss of podocytes would represent just one process that occurs *pari passu* with the other progressive aspects of renal injury. The correlations of podocyte loss with hypofiltration and sclerosis do not prove the existence of a causal relationship.

On the other hand, several mechanisms have been

described by which primary podocyte loss would be expected to lead to progressive renal dysfunction [21]. An inadequate number of podocytes may lead to increased occurrence of patches of "bare" GBM, raising the chances of formation of a synechia, the first committed lesion of segmental glomerular sclerosis. Podocytes are also determining components of the glomerular permselectivity barrier [22, 23]. It has been shown that such areas of denuded GBM are the sites at which macromolecular probes permeate into Bowman's space in rats with experimental podocyte injury [22, 24]. It is therefore conceivable that denuded areas of GBM represent the shunt-like, protein-permeable "pores" revealed by our analysis of Ficoll sieving in the IgA nephropathy patients, although this possibility was not explored in the current study.

Thus, it appears that podocyte loss could account for all three cardinal features of glomerular injury in IgA nephropathy: glomerular sclerosis leading to a loss of ultrafiltration capacity, an ensuing depression of GFR, and proteinuria. It has been proposed that proteinuria also contributes to the type of progressive interstitial fibrosis we observed by inducing tubular production of various chemotactic and inflammatory mediators [25, 26].

In this cross-sectional study we cannot distinguish whether podocytopenia in severe IgA nephropathy was due to a loss of podocytes in the course of the disease or whether the more severely affected subjects had a lower number of podocytes already at the onset of disease, perhaps predisposing them to a more aggressive form of glomerular injury. The studies of Hara and associates provide evidence of podocalyxin-positive cells (podocytes) in the urine of the vast majority of pediatric and adult patients with IgA nephropathy, but an absence of such cells in the urine of patients with nonglomerular hematuria as well as several other renal diseases [27]. These findings are consistent with an ongoing loss of podocytes into the urine of patients with IgA nephropathy. In addition, recent studies in Pima Indians with incipient type 2 diabetic nephropathy have demonstrated a significant loss of podocytes in the transition from microalbuminuric to macroalbuminuric stages of that disease [28].

We submit that whereas IgA nephropathy is initiated by intramesangial deposition of complement-activating IgA [29], it is possible that it is injury to, and loss of, podocytes from the outer aspect of the glomerular basement membrane that determines the severity of disease as well as its rate of progression. The mechanism by which an initially intramesangial process leads to podocyte loss remains to be elucidated. One possibility is that the terminal membrane attack complex of complement, C5b-9, produced in the mesangium reaches the podocyte in the primary glomerular filtrate [30], leading to disruption of the actin-based cytoskeleton of the podocyte [31]. Even if exposure to ultrafiltered complement complexes is insufficient to cause cell death in situ, it may cause sufficient injury to result in detachment of the podocyte from the basement membrane. Regardless of the precise mechanism resulting in podocytopenia, our data lead us to propose that below a threshold value of podocytes per glomerulus, a state of podocyte "insufficiency" ensues [32], leading to deterioration of glomerular function. We propose further that the mechanism by which podocyte insufficiency leads to glomerular dysfunction involves destabilization of the glomerular tuft, with subsequent loss of filtration and permselective properties and eventual tuft destruction through glomerular sclerosis.

ACKNOWLEDGMENTS

This study was supported by a grant from the National Institute of Diabetes and Digestive and Kidney Diseases (DK49372). During part of this study, Dr. Lemley was supported as a Clinical Associate Physician in the General Clinical Research Center at Stanford University (M01-RR-00070) and by a Faculty Scholar Award from Satellite Dialysis Corporation, Inc. Parts of this work have been presented in abstract form at the American Society of Nephrology, Miami, FL, November 6, 1999. The authors gratefully acknowledge the expert technical assistance of Ms. Catherine Polhemus, Dr. Michelle Hladunewich and Ms. Linda Anderson in the morphometric analysis.

Reprint requests to Kevin V. Lemley, M.D., Ph.D., Division of Pediatric Nephrology, Room G306, Stanford University Medical Center, Stanford, California 94305-5208, USA
E-mail: klemley@stanford.edu

REFERENCES

1. Rychlik I, Andrassy K, Waldherr R, *et al*: Clinical features and natural history of IgA nephropathy. *Ann Med Interne (Paris)* 150:117–126, 1999
2. D'Amico G: Influence of clinical and histological features on actuarial renal survival in adult patients with idiopathic IgA nephropathy, membranous nephropathy, and membranoproliferative glomerulonephritis: Survey of the recent literature. *Am J Kidney Dis* 20:315–323, 1992
3. Nomoto Y, Endoh M, Suga T, *et al*: Minimum requirements for renal biopsy size for patients with IgA nephropathy. *Nephron* 60:171–175, 1992
4. Battilana C, Zhang HP, Olshen RA, *et al*: PAH extraction and estimation of plasma flow in diseased human kidneys. *Am J Physiol* 261:F726–F733, 1991
5. Canaan-Kuhl S, Venkatraman ES, Ernst SI, *et al*: Relationships among protein and albumin concentrations and oncotic pressure in nephrotic plasma. *Am J Physiol* 264:F1052–F1059, 1993
6. Nakamura Y, Myers BD: Charge selectivity of proteinuria in diabetic glomerulopathy. *Diabetes* 37:1202–1211, 1988
7. Blouch K, Deen WM, Fauvel JP, *et al*: Molecular configuration and glomerular size selectivity in healthy and nephrotic humans. *Am J Physiol* 273:F430–F437, 1997
8. Bohrer MP, Deen WM, Robertson CR, *et al*: Influence of molecular configuration on the passage of macromolecules across the glomerular capillary wall. *J Gen Physiol* 74:583–593, 1979
9. Deen WM, Bridges CR, Brenner BM, Myers BD: Heteroporous model of glomerular size selectivity: Application to normal and nephrotic humans. *Am J Physiol* 249:F374–F389, 1985
10. Drumond MC, Kristal B, Myers BD, Deen WM: Structural basis for reduced glomerular filtration capacity in nephrotic humans. *J Clin Invest* 94:1187–1195, 1994
11. Weibel ER: *Stereologic Methods. Practical Methods for Biological Morphometry.* London, Academic Press, Inc., 1979, 415 pp
12. Miller PL, Meyer TW: Effects of tissue preparation on glomer-

ular volume and capillary structure in the rat. *Lab Invest* 63:862–866, 1990
13. Gundersen HJ: Notes on the estimation of the numerical density of arbitrary profiles: The edge effect. *J Microsc* 111:219–223, 1977
14. Pagtalunan ME, Miller PL, Jumping-Eagle S, *et al*: Podocyte loss and progressive glomerular injury in type II diabetes. *J Clin Invest* 99:342–348, 1997
15. Jensen EB, Gundersen HJ, Østerby R: Determination of membrane thickness distribution from orthogonal intercepts. *J Microsc* 115:19–33, 1979
16. Squarer A, Lemley KV, Ambalavanan S, *et al*: Mechanisms of progressive glomerular injury in membranous nephropathy. *J Am Soc Nephrol* 9:1389–1398, 1998
17. Drumond MC, Deen WM: Structural determinants of glomerular hydraulic permeability. *Am J Physiol* 266:F1–F12, 1994
18. Deen WM, Robertson CR, Brenner BM: Concentration polarization in an ultrafiltering capillary. *Biophys J* 14:412–431, 1974
19. Deen WM, Robertson CR, Brenner BM: A model of glomerular ultrafiltration in the rat. *Am J Physiol* 223:1178–1183, 1972
20. Kriz W, Gretz N, Lemley KV: Progression of glomerular diseases: is the podocyte the culprit? *Kidney Int* 54:687–697, 1998
21. Kriz W, Lemley KV: The role of the podocyte in glomerulosclerosis. *Curr Opin Nephrol Hypertens* 8:489–497, 1999
22. Laurens W, Battaglia C, Foglieni C, *et al*: Direct podocyte damage in the single nephron leads to albuminuria in vivo. *Kidney Int* 47:1078–1086, 1995
23. Daniels BS, Deen WM, Mayer G, *et al*: Glomerular permeability barrier in the rat. Functional assessment by in vitro methods. *J Clin Invest* 92:929–936, 1993
24. Kanwar YS, Rosenzweig LJ: Altered glomerular permeability as a result of focal detachment of the visceral epithelium. *Kidney Int* 21:565–574, 1982
25. Kees-Folts D, Sadow JL, Schreiner GF: Tubular catabolism of albumin is associated with the release of an inflammatory lipid. *Kidney Int* 45:1697–1709, 1994
26. Remuzzi G, Ruggenenti P, Benigni A: Understanding the nature of renal disease progression. *Kidney Int* 51:2–15, 1997
27. Hara M, Yamamoto T, Yanagihara T, *et al*: Urinary excretion of podocalyxin indicates glomerular epithelial cell injuries in glomerulonephritis. *Nephron* 69:397–403, 1995
28. Lemley KV, Blouch K, Abdullah I, *et al*: Glomerular permselectivity at the onset of nephropathy in type 2 diabetes mellitus. *J Am Soc Nephrol* 11:2095–2105, 2000
29. Morita Y, Ikeguchi H, Nakamura J, *et al*: Complement activation products in the urine from proteinuric patients. *J Am Soc Nephrol* 11:700–707, 2000
30. Rauterberg EW, Lieberknecht HM, Wingen AM, Ritz E: Complement membrane attack (MAC) in idiopathic IgA-glomerulonephritis. *Kidney Int* 31:820–829, 1987
31. Topham PS, Haydar SA, Kuphal R, *et al*: Complement-mediated injury reversibly disrupts glomerular epithelial cell actin microfilaments and focal adhesions. *Kidney Int* 55:1763–1775, 1999
32. Fries JW, Sandstrom DJ, Meyer TW, Rennke HG: Glomerular hypertrophy and epithelial cell injury modulate progressive glomerulosclerosis in the rat. *Lab Invest* 60:205–218, 1989